Reinvestigation of the Reaction of $(NH_4)_2[Ce(NO_3)_6]$ with Triphenylphosphine Oxide; the Crystal Structure and Magnetic Properties of mer-$Ce(NO_3)_3(OPPh_3)_3 \cdot 2(CH_3)_2CO$

Jianhua Lin, Evamarie Hey-Hawkins, and Hans Georg von Schnering
Max-Planck-Institut für Festkörperforschung, Stuttgart

Z. Naturforsch. **45a**, 1241–1247 (1990); received September 18, 1990

Professor Dirk Reinen zum 60. Geburtstag gewidmet

The reaction of $(NH_4)_2[Ce(NO_3)_6]$ with two equivalents of $OPPh_3$ (Ph = C_6H_5) in acetonitrile yields $Ce(NO_3)_4(OPPh_3)_2$ (**1**) in high yield, whereas using acetone as solvent affords mer-$Ce(NO_3)_3(OPPh_3)_3 \cdot 2(CH_3)_2CO$ (**2**), the yield of which is dependent on the reaction time. A crystal structure determination of **2** shows that the Ce atom is coordinated with three bidentate nitrato groups and three $OPPh_3$ ligands, thus achieving a coordination number of nine. Eight non-coordinating acetone molecules are present in the unit cell. Crystal data (292 K): space group $P2_1/n$ (no. 14), $a = 12.438$ (2), $b = 25.532$ (4), $c = 20.379$ (4) Å, $\beta = 96.33$ (2)°, $V = 6432$ (1) Å, $Z = 4$, $d_{calc} = 1.318$ g cm^{-3}. Due to poor crystal quality the refinement converges at $R = 0.11$, $R_w = 0.09$. **2** is paramagnetic, but it does not follow the Curie-Weiss law at low temperature. Therefore crystal field theory was used in order to explain these findings.

Key words: Mer-trinitratotris(triphenylphosphine oxide) cerium(III) di-acetone adduct, crystal structure, magnetic properties, tetranitratobis(triphenylphosphine oxide) cerium(IV).

Introduction

A large number of formally Ce(III) and Ce(IV) complexes is known. Although numerous magnetic studies of Ce(III) complexes have been reported, hardly any investigations of Ce(IV) compounds have been undertaken, as it seems to be obvious that a Ce(IV) complex should not exhibit any paramagnetic properties.

A theoretical study by Neumann and Fulde [1] suggests that $Ce(COT)_2$ (COT = cyclooctatetraene dianion), which contains Ce with a formal valency of +4, may form a ground state resembling a Kondo singlet. The experimental consequence would be that $Ce(COT)_2$ should exhibit a van Vleck-type paramagnetism at low temperature.

Besides this it is of interest to examine other inorganic or organometallic compounds of formally Ce(IV) to determine whether the unusual magnetic behaviour proposed for $Ce(COT)_2$ is observable in these complexes.

We now report an improved synthesis of $Ce(NO_3)_4(OPPh_3)_2$ (**1**) (Ph = C_6H_5) as well as the synthesis and X-ray structure determination of mer-$Ce(NO_3)_3(OPPh_3)_3 \cdot 2(CH_3)_2CO$ (**2**). Complex **2** was obtained in high yield using a literature procedure for the synthesis of $Ce(NO_3)_4(OPPh_3)_2$ (**1**) [2].

Reprint requests to Dr. E. Hey-Hawkins, Max-Planck-Institut für Festkörperforschung, Heisenbergstraße 1, Postfach 80 06 65, D-7000 Stuttgart 80.

Synthesis of 1 and 2

According to Caughlan et al. [2], **1** can be obtained from $(NH_4)_2[Ce(NO_3)_6]$ and two equivalents of $OPPh_3$ in acetone. The recrystallisation of **1** from acetonitrile was, however, accompanied by considerable losses due to reduction to a Ce(III) compound, which they did not characterise. In our hands, prolonged reaction (12 h) in acetone led exclusively to formation of **2**. However, when acetonitrile was used as the solvent **1** was obtained in high yield and could be recrystallised from acetonitrile with negligible loss. Shortening the reaction time to 1 h and using acetone as a solvent afforded solid NH_4NO_3 and a yellow solution. Separation and concentration of this solution yielded an oily yellow residue which was extracted several times with acetonitrile. Cooling the resulting CH_3CN solution to −30 °C gave small amounts of yellow, crystalline **1**, whose elemental

0932-0784 / 90 / 1100-1241 $ 01.30/0. – Please order a reprint rather than making your own copy.

analysis, spectroscopic data, and unit cell parameters were in agreement with those reported previously [2].

The residual solid, which is insoluble in CH_3CN, dissolves readily in acetone. Cooling of this solution to $-30\,^{\circ}C$ affords **2** as pale yellow crystals. Recrystallisation of these pale yellow crystals from acetone afforded colourless crystals, the melting point, i.r. spectrum, and analytical data of which are identical to those observed for the pale yellow crystals of **2**, and those reported previously [3].

The reduction mechanism is as yet uncertain, but we feel that acetone seems to facilitate a redox process being itself oxidised. The resulting Ce(III) compound could then react with $OPPh_3$ to yield **2**. This assumption is supported by the fact that the sticky yellow solid obtained on evaporation of the acetone always smells of nitric acid. The Ce(IV) complex itself is thermally stable up to the 170 °C. In the mass spectrum a peak for NO_2 (m/e 46) is observed only at elevated temperature (above 170 °C).

Crystal Structure of 2

An X-ray crystal structure determination was carried out on a single crystal of **2** (pale yellow material). Table 1 summarises the details of the data collection and structure solution, Table 2 lists the bond lengths and angles, and Table 3 gives the positional and thermal parameters *.

2 crystallises monoclinic in the space group $P2_1/n$ (no. 14) with the cell parameters (292 K), $a = 12.438\,(2)$, $b = 25.532\,(4)$, $c = 20.379\,(4)$ Å, $\beta = 96.33\,(2)^{\circ}$ and $Z = 4$ formula units. The Ce atom is coordinated by the oxygen atoms of three bidentate nitrato groups and of three $OPPh_3$ ligands, and thus achieves a coordination number of nine (Figure 1). If each NO_3 group is considered to occupy only one coordination site, the coordination can be described as a distorted octahedron in which two trans oriented $OPPh_3$ ligands occupy the axial positions. The Ce–O(NO_3) distances range from 2.58 (1) to 2.63 (1) Å, while the Ce–O($OPPh_3$) bonds are shorter [2.39 (1)–2.42 (1) Å]. The terminal N–O distances are comparable to the N–O(Ce) bond lengths [range 1.25 (2)–1.28 (3) Å].

* Further details of the structure determination have been deposited as Supplementary Publication No. CSD 54886. Copies may be obtained from the Fachinformationszentrum Energie, Physik, Mathematik, D-7514 Eggenstein-Leopoldshafen 2.

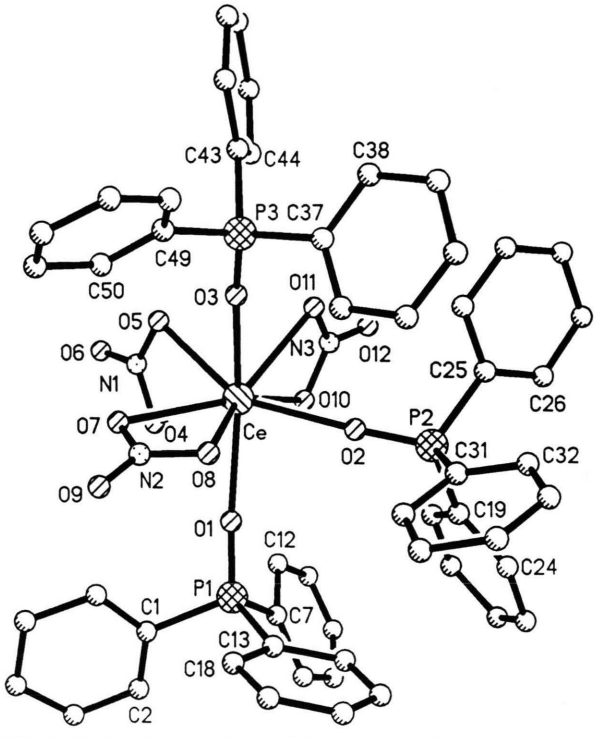

Fig. 1. Molecular structure of the mer-$Ce(NO_3)_3(OPPh_3)_3$ molecule in **2** showing the atomic numbering scheme employed. H atoms are omitted for clarity.

Table 1. Details of the data collection and structure determination for $Ce(NO_3)_3(OPPh_3)_3 \cdot 2(CH_3)_2CO$.

Formula	$C_{60}H_{57}O_{14}N_3P_3Ce$; mole mass: 1277.15 [amu]
Unit cell	Temperature 295 K, monoclinic, $P2_1/n$ (no. 14), $a = 12.438\,(2)$ Å, $b = 25.532\,(4)$ Å, $c = 20.379\,(4)$ Å, $\beta = 96.33\,(2)^{\circ}$, $Z = 4$, $V = 6432\,(1)$ Å^3
Density	$d_{cal} = 1.318$ g cm^{-3}
Data collection	Diffractometer Nicolet R3m/v, graphite monochromator, scintillation counter, $\lambda(MoK_\alpha) = 0.71069$ Å, Wyckoff scan, 11386 unique reflections, 7224 with $F \geq 3\sigma(F)$, empirical absorption correction with 12 reflections, $\mu(MoK_\alpha) = 7.63$ cm^{-1}
Structure determination	Patterson methods, refinement with SHELX-76, full matrix, least squares, 112 parameters, Ce, P1–P3, N1–N3, O1–O12 anisotropic, all other atoms isotropic, H atoms in calculated positions (C–H = 1.08 Å), weight: $1\,(\sigma(F))^{-2}$ R (aniso) = 0.110, R_w (aniso) = 0.090.

The coordination of the Ce atom as well as the observed bond distances and angles of **2** are similar to those reported for **1** [2]. In **1**, the two $OPPh_3$ ligands are in a trans arrangement, O–Ce–O being 155.0 (3)°, while the four nitrato ligands are oriented in the shape

Table 2. Bond lenghts (Å) and bond angles (degree) in **2** (standard deviations).

Ce–O1	2.41 (1)	O2–Ce–O8	80.0 (4)
Ce–O2	2.42 (1)	O2–Ce–O10	77.3 (4)
Ce–O3	2.39 (1)	O2–Ce–O11	76.2 (4)
Ce–O4	2.64 (1)	O3–Ce–O4	125.1 (4)
Ce–O5	2.58 (1)	O3–Ce–O5	79.6 (4)
Ce–O7	2.60 (2)	O3–Ce–O7	82.2 (4)
Ce–O8	2.63 (1)	O3–Ce–O8	76.4 (4)
Ce–O10	2.58 (1)	O3–Ce–O10	121.5 (4)
Ce–O11	2.60 (1)	O3–Ce–O11	72.9 (4)
P1–O1	1.48 (1)	O4–Ce–O5	47.6 (4)
P2–O2	1.48 (1)	O4–Ce–O7	73.8 (5)
P3–O3	1.50 (1)	O4–Ce–O8	117.6 (5)
N1–O4	1.24 (2)	O4–Ce–O10	72.7 (5)
N1–O5	1.27 (2)	O4–Ce–O11	100.7 (5)
N1–O6	1.22 (2)	O5–Ce–O7	77.2 (5)
N2–O7	1.27 (3)	O5–Ce–O8	123.8 (5)
N2–O8	1.30 (3)	O5–Ce–O10	83.8 (4)
N2–O9	1.23 (3)	O5–Ce–O11	74.4 (5)
N3–O10	1.26 (2)	O7–Ce–O8	49.9 (5)
N3–O11	1.25 (3)	O7–Ce–O10	146.2 (4)
N3–O12	1.22 (2)	O7–Ce–O11	144.9 (5)
P1–C1	1.81 (2)	O8–Ce–O10	151.1 (4)
P1–C7	1.84 (2)	O8–Ce–O11	140.2 (5)
P1–C13	1.79 (2)	O10–Ce–O11	48.7 (4)
P2–C19	1.81 (2)	O6–N1–O4	122 (2)
P2–C25	1.79 (2)	O6–N1–O5	125 (2)
P2–C31	1.79 (2)	O4–N1–O5	114 (2)
P3–C37	1.80 (2)	O9–N2–O7	124 (2)
P3–C43	1.80 (2)	O9–N2–O8	118 (2)
P3–C49	1.80 (2)	O7–N2–O8	118 (2)
O1–Ce–O2	82.7 (4)	O12–N3–O11	123 (2)
O1–Ce–O3	152.6 (4)	O12–N3–O10	120 (2)
O1–Ce–O4	70.2 (4)	O11–N3–O10	117 (2)
O1–Ce–O5	117.4 (4)	P1–O1–Ce	174.0 (8)
O1–Ce–O7	81.2 (4)	P2–O2–Ce	171.4 (7)
O1–Ce–O8	76.2 (4)	P3–O3–Ce	171.6 (7)
O1–Ce–O10	83.4 (4)	N1–O4–Ce	98 (1)
O1–Ce–O11	130.5 (4)	N1–O5–Ce	100 (1)
O2–Ce–O3	91.4 (4)	N2–O7–Ce	97 (1)
O2–Ce–O4	141.3 (4)	N2–O8–Ce	95 (1)
O2–Ce–O5	150.6 (4)	N3–O10–Ce	98 (1)
O2–Ce–O7	129.7 (4)	N3–O11–Ce	97 (1)

Mean bond distances and bond angles of the triphenylphosphine oxide ligands

$\overline{C–C}$	1.38	(3)
$\overline{C–C–C}$	118	(2)
$\overline{O–P–C}$	111.4	(8)
$\overline{C–P–C}$	107.5	(8)
$\overline{C–C–P}$	120	(1)
Acetone		
C55–O13	1.24	(4)
C55–C57	1.47	(5)
C55–C56	1.48	(4)
C58–O14	1.25	(4)
C58–C60	1.38	(4)
C58–C59	1.47	(4)
O13–C55–C57	120	(3)
O13–C55–C56	124	(3)
C57–C55–C56	116	(3)
O14–C58–C60	111	(3)
O14–C58–C59	124	(3)
C60–C58–C59	125	(3)

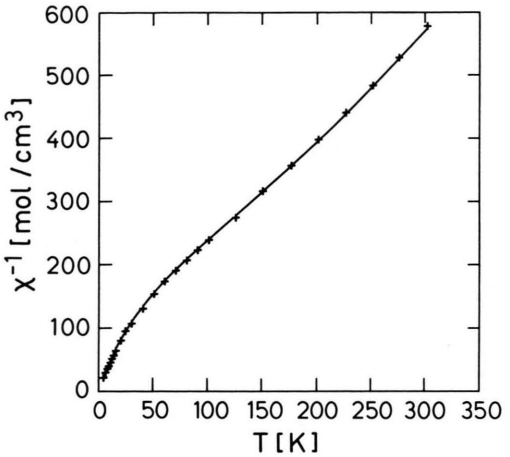

Fig. 2. Temperature dependence of the reciprocal magnetic susceptibility ($1/\chi_{mol}$) of **2**. *** experimental values; —— best fit calculation assuming mm2-C_{2v} symmetry.

of a four-bladed propeller. In **2** two of the three $OPPh_3$ ligands show a trans arrangement [O–Ce–O 152.6(4)°], while one of the four nitrato groups in **1** is displaced by a $OPPh_3$ ligand. In **1** there are rather unfavourable short O ··· O contacts. Replacement of one of the four NO_3 groups in **1** by $OPPh_3$ leads to less ligand-ligand repulsion. This could account for the observed instability of **1** in certain solvents with respect to formation of **2**, in which the Ce atom is in a less crowded environment.

Magnetic Properties of 1 and 2

The magnetic susceptibility of compounds **1** and **2** was measured with a SQUID magnetometer in the temperature range 4.6 to 300 K. Over the whole temperature range, **1** shows diamagnetic behaviour with a temperature dependence that is believed to be due to impurities (Ce^{3+}) in the sample. Compound **2** is paramagnetic, but it does not follow the Curie-Weiss law at low temperature (Figure 2). In order to explain these findings we used crystal field theory to calculate the magnetic susceptibility of **2**.

Owing to the large spin-orbit coupling, the excited state of Ce^{3+} ($^2F_{7/2}$) lies far above the ground state ($^2F_{5/2}$). The separation between these two states of about 2000–2500 cm^{-1} is much greater than the crystal field splitting, so that only the crystal field splitting of the ground state need be considered.

In compound **2**, the point symmetry is 1-C_1, as shown in Figure 1. However, to simplify the calculation, a higher symmetry was chosen. As an approximation, only the interactions between oxygen atoms and Ce^{3+} were considered, and the intercept of the planes O2-Ce-O7 and O1-Ce-O3 was taken as the Z axis. The X axis lies in the O1-Ce-O3 plane, and the Y axis is perpendicular to X and Z. In addition, all oxygen atoms were assumed to be equivalent. From Fig. 1 it can be seen that if the angles O4-Ce-O5 and O4-Ce-O10 are taken to be equal and the distortion of O8 from the Z axis is disregarded, **2** has the local symmetry 4 mm-C_{4v}. The distortion of oxygen atoms other than O8 from 4 mm-C_{4v} symmetry leads to mm 2-C_{2v} symmetry. Therefore, in our calculation we used 4 mm-C_{4v} symmetry as a first approximation and treated the distortion of the coordinated oxygen atoms from 4 mm-C_{4v} symmetry as a mm 2-C_{2v} perturbation. For the distortion of O8 from mm 2-C_{2v} symmetry, however, the calculation based on the point charge model shows that it has only a small influence on the energy splitting ($B_{21}/B_{20}=0.05$) and it can therefore be ignored in the calculation.

For full details on our calculations refer to Appendix 1. A short summary as well as the results obtained will be given here.

By considering the crystal field and the magnetic field, the crystal field splitting and the Zeeman energy of the Ce^{3+} in compound **1** can be obtained as a function of the crystal field intensity parameter B_{kq} (cf. Appendix 1). Therefore, the magnetic susceptibility can be calculated by using the van Vleck equation:

$$\chi_{mol}=\chi_{cf}+\chi_d = -\frac{(N/H)\cdot\sum_i(\delta E_i/\delta H)\cdot\exp(-E_i/kT)}{\sum_i\exp(-E_i/kT)}+d. \quad (1)$$

The calculated magnetic susceptibility was fitted with the experimental values using the method of least-squares. In this method the five crystal field intensity parameters as well as the diamagnetic contribution of each molecule χ_d were refined.

Figure 2 shows the measured $1/\chi_{mol}$ values and the calculated curve resulting from the best fit. From the best fit calculation, the values of the five crystal field intensity parameters B_{kq} and the diamagnetic contribution χ_d can be obtained. The diamagnetic contribution of the molecule, deduced from the best fit calculation is about $-1.1\cdot10^{-3}$ cm^3 mol^{-1}, which can be compared to the value of about $-0.75\cdot10^{-3}$ cm^3 mol^{-1} calculated from the incremental model (see Appendix, Table A1). Furthermore, from the parameters B_{kq}, the coefficients a_i of the eigenstates in (A11) (Appendix 1) can be obtained; hence, the perturbation eigenstates can be expressed as follows:

$$\Phi_1=0.534|\pm5/2\rangle+0.844|\mp3/2\rangle-0.042|\pm1/2\rangle,$$
$$\Phi_2=0.706|\pm5/2\rangle-0.588|\mp3/2\rangle-0.396|\pm1/2\rangle, \quad (2)$$
$$\Phi_3=0.326|\pm5/2\rangle-0.221|\mp3/2\rangle+0.919|\pm1/2\rangle.$$

Consideration of the parameters in Table A2 shows first of all that Φ_1 is the ground state since E_2-E_1 and E_3-E_1 have positive values. The next state, Φ_2, lies 126 cm^{-1} above the ground state. The highest state, Φ_3, is located 309 cm^{-1} above the ground state (Figure 3). This splitting can be compared with the corresponding values based on the point charge model. The crystal field intensity parameters can be calculated from the ligand sum A_{kq}, the radial integral $\langle r^k\rangle$, and the Stevens multiplicative factor Θ_k. In this calculation we only consider the interactions between oxygen atoms and Ce^{3+} and assume that all the oxygen ions have a charge of $-1/3$. The lattice sum A_{kq} was calculated from the relative positions of Ce^{3+} and the oxygen atoms in Table 3, the radial integral $\langle r^k\rangle$ and Stevens multiplicative factor Θ_k were taken from the references [4, 5]. The results of applying this model are shown in the second column of Table A2 (Appendix 1). The energy levels calculated from the point

Table A1. Calculation of the diamagnetic susceptibility χ_d with the incremental model [10].

Component	χ_d (cm$^3\cdot$mol^{-1})
2 CH_3COCH_3	$2(-35\cdot10^{-6})$
Ce^{3+}	$-20\cdot10^{-6}$
3 NO_3^-	$3(-20\cdot10^{-6})$
3 $OPPh_3$	$3(-200\cdot10^{-6})$
SUM	$-7.5\cdot10^{-4}$

Table A2. Parameters obtained from the best fit calculation (a) and from the point charge model (b).

		(a)	(b)
Crystal field parameters (cm^{-1})	B_{20}	−4.86	−6.49
	B_{40}	0.83	0.19
	B_{44}	1.19	−0.98
	B_{22}	3.13	1.79
	B_{42}	1.65	0.71
The energy separation (cm^{-1})	E_2-E_1	126	43
	E_3-E_1	309	182

Table 3. Positional parameters and thermal parameters (pm^2) in **2** (standard deviations).

Atom	*x*	*y*	*z*	$U_{iso/equi}$
Ce	0.7507 (1)	0.19840 (4)	0.25597 (5)	339 (3)
P1	0.9629 (4)	0.0968 (2)	0.3287 (2)	403 (16)
P2	1.0120 (4)	0.2715 (2)	0.2194 (2)	438 (17)
P3	0.6065 (4)	0.3318 (2)	0.2736 (2)	424 (17)
N1	0.571 (1)	0.1184 (7)	0.215 (1)	666 (77)
N2	0.737 (2)	0.2027 (8)	0.403 (1)	771 (95)
N3	0.759 (1)	0.1994 (9)	0.1085 (8)	655 (79)
O1	0.877 (1)	0.1328 (5)	0.3007 (5)	519 (48)
O2	0.9147 (9)	0.2454 (4)	0.2397 (6)	480 (44)
O3	0.653 (1)	0.2785 (4)	0.2630 (6)	491 (45)
O4	0.662 (1)	0.1047 (5)	0.2404 (8)	753 (61)
O5	0.557 (1)	0.1679 (6)	0.2136 (7)	736 (59)
O6	0.500 (1)	0.0866 (6)	0.198 (1)	1158 (88)
O7	0.667 (1)	0.1783 (6)	0.3646 (7)	669 (61)
O8	0.808 (1)	0.2305 (6)	0.3771 (6)	681 (60)
O9	0.743 (2)	0.2003 (9)	0.4638 (7)	1353 (102)
O10	0.798 (1)	0.1624 (5)	0.1442 (6)	576 (53)
O11	0.713 (1)	0.2352 (6)	0.1369 (7)	642 (59)
O12	0.772 (1)	0.2009 (7)	0.0500 (6)	1016 (77)
C1	0.909 (1)	0.0492 (7)	0.3825 (8)	425 (41)
C2	0.961 (2)	0.0042 (7)	0.3941 (9)	531 (50)
C3	0.919 (2)	−0.0310 (8)	0.439 (1)	702 (62)
C4	0.827 (2)	−0.0192 (8)	0.470 (1)	733 (64)
C5	0.775 (2)	0.027 (1)	0.457 (1)	932 (80)
C6	0.818 (2)	0.0607 (8)	0.412 (1)	690 (60)
C7	1.020 (1)	0.0607 (7)	0.2624 (8)	457 (45)
C8	1.122 (2)	0.0391 (7)	0.271 (1)	640 (60)
C9	1.150 (2)	0.0144 (8)	0.214 (1)	775 (67)
C10	1.087 (2)	0.0082 (8)	0.158 (1)	655 (59)
C11	0.995 (2)	0.0271 (8)	0.152 (1)	649 (58)
C12	0.957 (1)	0.0547 (7)	0.2025 (9)	563 (49)
C13	1.070 (1)	0.1308 (6)	0.3773 (8)	445 (45)
C14	1.159 (2)	0.1493 (7)	0.3507 (9)	593 (55)
C15	1.236 (2)	0.1800 (8)	0.389 (1)	755 (67)
C16	1.220 (2)	0.1935 (8)	0.450 (1)	711 (58)
C17	1.134 (2)	0.1777 (8)	0.478 (1)	674 (61)
C18	1.055 (2)	0.1448 (7)	0.4410 (9)	567 (52)
C19	1.109 (1)	0.2237 (7)	0.1974 (8)	470 (46)
C20	1.076 (2)	0.1801 (7)	0.1630 (9)	549 (53)
C21	1.151 (2)	0.1419 (9)	0.148 (1)	764 (66)
C22	1.261 (2)	0.1504 (8)	0.167 (1)	733 (64)
C23	1.299 (2)	0.1935 (9)	0.2020 (9)	733 (60)
C24	1.222 (2)	0.2326 (8)	0.217 (1)	675 (59)
C25	0.980 (1)	0.3118 (7)	0.1480 (8)	466 (46)
C26	1.042 (2)	0.3124 (8)	0.097 (1)	730 (63)
C27	1.015 (2)	0.3462 (9)	0.040 (1)	790 (74)
C28	0.924 (2)	0.3771 (9)	0.040 (1)	845 (72)
C29	0.871 (2)	0.377 (1)	0.094 (1)	941 (79)
C30	0.893 (2)	0.3427 (7)	0.1482 (9)	607 (55)
C31	1.078 (1)	0.3121 (6)	0.2836 (8)	433 (44)
C32	1.137 (2)	0.3546 (8)	0.272 (1)	684 (62)
C33	1.198 (2)	0.3798 (9)	0.321 (1)	805 (69)
C34	1.192 (2)	0.364 (1)	0.380 (1)	916 (80)
C35	1.133 (2)	0.3204 (9)	0.397 (1)	851 (76)
C36	1.073 (2)	0.2963 (8)	0.3474 (9)	580 (51)
C37	0.708 (1)	0.3820 (6)	0.2754 (8)	409 (43)
C38	0.693 (2)	0.4296 (7)	0.2417 (9)	561 (53)
C39	0.773 (2)	0.4688 (8)	0.249 (1)	797 (70)
C40	0.871 (2)	0.4603 (8)	0.289 (1)	747 (65)
C41	0.885 (2)	0.4124 (8)	0.320 (1)	691 (60)
C42	0.804 (2)	0.3740 (7)	0.3144 (9)	580 (53)
C43	0.500 (1)	0.3461 (6)	0.2089 (8)	422 (44)
C44	0.490 (2)	0.3148 (7)	0.1538 (9)	606 (56)
C45	0.406 (2)	0.3259 (8)	0.100 (1)	731 (65)

Table 3 (continued).

Atom	*x*	*y*	*z*	$U_{iso/equi}$
C46	0.334 (2)	0.3674 (8)	0.103 (1)	613 (58)
C47	0.348 (2)	0.3993 (7)	0.1623 (9)	572 (53)
C48	0.427 (1)	0.3878 (7)	0.2151 (9)	523 (50)
C49	0.548 (1)	0.3376 (7)	0.3502 (8)	475 (47)
C50	0.513 (2)	0.2917 (8)	0.378 (1)	702 (63)
C51	0.473 (2)	0.297 (1)	0.438 (1)	879 (71)
C52	0.470 (2)	0.344 (1)	0.466 (1)	917 (85)
C53	0.507 (2)	0.3910 (8)	0.442 (1)	689 (61)
C54	0.547 (2)	0.3855 (7)	0.3823 (9)	594 (54)
O13	0.449 (2)	0.108 (1)	−0.009 (1)	1782 (98)
C55	0.402 (3)	0.148 (1)	0.007 (1)	1102 (94)
C56	0.459 (3)	0.193 (1)	0.040 (1)	1507 (120)
C57	0.284 (3)	0.153 (1)	−0.009 (2)	1711 (144)
O14	0.318 (2)	0.4858 (8)	0.495 (1)	1425 (76)
C58	0.218 (3)	0.484 (1)	0.498 (1)	1090 (93)
C59	0.136 (2)	0.497 (1)	0.443 (1)	1244 (102)
C60	0.195 (3)	0.468 (1)	0.560 (1)	1588 (140)

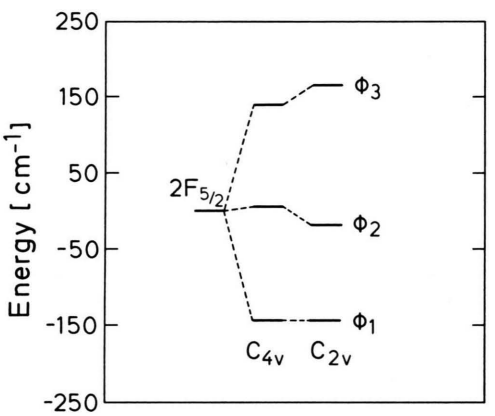

Fig. 3. Crystal field splitting of the $^2F_{5/2}$ level in a crystal field of 4mm-C_{4v} or mm2-C_{2v} symmetry.

charge model are of the same order as those obtained from the best fit calculation, but the energy separation is much smaller (about 60%). This means that only 60% of the crystal field splitting found experimentally can be explained by the simple ionic model. The additional crystal field splitting may represent the covalent contribution of the Ce–O bonds or an other charge distribution of the oxygen atoms. By considering crystal field splitting and magnetic exchange, Lueken et al. [6] have fitted the susceptibility of $NaCeS_2$ with cubic symmetry. They obtained a splitting between the doublet ground state and the quartet state of about 470 cm^{-1} and found that the covalent contribution to the crystal field splitting is about 36%. This is comparable with our results.

Appendix 1

1. Crystal Field Splitting

The crystal field Hamiltonian $\hat{H}_{CF}$ of an f electron, in the general form [7, 8], is given by the equation

$$\hat{H}_{CF}=\sum_{k}\sum_{q=0}^{k} B_{kq}\hat{O}_{kq} \quad \text{with} \quad k=0, 2, 4, 6. \quad (A1)$$

The term $\hat{O}_{kq}$ represents the operator equivalents in the notation of Stevens [8]. The crystal field intensity parameters B_{kq} are given by

$$B_{kq}=k\,\Theta_k\langle r^k\rangle A_{kq}, \quad (A2)$$

where Θ_k is the Stevens multiplicative factor and $\langle r^k\rangle A_{kq}$ the crystal field parameter [4]. The term $\langle r^k\rangle A_{kq}$ consists of the radial integral $\langle r^k\rangle$ multiplied by the ligand sum A_{kq}, which in turn depends on the charges and positions of the atoms in the crystal. For the $^2F_{5/2}$ state, sixth order terms ($k=6$) vanish since $\Theta_6=0$ [4]. Since the terms with $k=0$ will shift all energy levels by the same amount and do not contribute to the crystal field splitting, these terms can also be ignored in the calculation. For C_{2v} symmetry, the crystal field Hamiltonian has the form

$$\hat{H}_{CF}=B_{20}\hat{O}_{20}+B_{40}\hat{O}_{40}+B_{44}\hat{O}_{44}+B_{22}\hat{O}_{22}+B_{42}\hat{O}_{42}. \quad (A3)$$

To obtain the eigenvalues and the eigenstates using perturbation theory the crystal Hamiltonian was divided into two parts, H_{C4v} and H_{C2v}, with H_{C2v} considered a perturbation of H_{C4v}:

$$\hat{H}_{C4v}=B_{20}\hat{O}_{20}+B_{40}\hat{O}_{40}+B_{44}\hat{O}_{44},$$
$$\hat{H}_{C2v}=B_{22}\hat{O}_{22}+B_{42}\hat{O}_{42}. \quad (A4)$$

A crystal field of C_{4v} symmetry leads to a splitting of the state $J=5/2$ into three doublets (Figure 3). The eigenstates are

$$\Phi_{10}=c_1|\pm 5/2\rangle+c_2|\mp 3/2\rangle,$$
$$\Phi_{20}=c_3|\pm 5/2\rangle+c_4|\mp 3/2\rangle, \quad (A5)$$
$$\Phi_{30}=|\pm 1/2\rangle.$$

In these equations, the terms c_i are functions of B_{20}, B_{40} and B_{44}. The eigenvalues of the sub-levels in 4 mm-C_{4v} symmetry can be obtained by solving the secular equations:

$$E_{10}=4\,B_{20}-60\,B_{40}-\{(6\,B_{20}+120\,B_{40})^2+720\,B_{44}^2\}^{1/2},$$
$$E_{20}=4\,B_{20}-60\,B_{40}+\{(6\,B_{20}+120\,B_{40})^2+720\,B_{44}^2\}^{1/2}, \quad (A6)$$
$$E_{30}=-8\,B_{20}+120\,B_{40}.$$

Since C_{4v} point symmetry has already removed all of the degeneracy of the $^2F_{5/2}$ state, except Kramers degeneracy, the C_{2v} distortion only influences the position of energy levels because the eigenstates are mixed under the C_{2v} Hamiltonian (Figure 3).

According to Rayleigh-Schrödinger perturbation theory, the first-order correction of the C_{4v} eigenstates due to H_{C2v} are

$$E_{i1}=\langle\Phi_{i0}|\hat{H}_{C2v}|\Phi_{i0}\rangle. \quad (A7)$$

These are all zero in this case. The second-order correction can be calculated from

$$E_{i2}=\sum_{j}|\langle\Phi_{i0}|\hat{H}_{C2v}|\Phi_{j0}\rangle|^2/(E_{i0}-E_{j0}). \quad (A8)$$

They have the values

$$E_{12}=-\frac{\{(\sqrt{10}\,c_1+3\sqrt{2}\,c_2)\,B_{22}+(9\sqrt{10}\,c_1-15\sqrt{2}\,c_2)\,B_{42}\}^2}{(E_{30}-E_{10})},$$

$$E_{22}=-\frac{\{(\sqrt{10}\,c_3+3\sqrt{2}\,c_4)\,B_{22}+(9\sqrt{10}\,c_3-15\sqrt{2}\,c_4)\,B_{42}\}^2}{(E_{30}-E_{20})},$$

$$E_{32}=\frac{\{(\sqrt{10}\,c_1+3\sqrt{2}\,c_2)\,B_{22}+(9\sqrt{10}\,c_1-15\sqrt{2}\,c_2)\,B_{42}\}^2}{(E_{30}-E_{10})}+\frac{\{(\sqrt{10}\,c_3+3\sqrt{2}\,c_4)\,B_{22}+(9\sqrt{10}\,c_3-15\sqrt{2}\,c_2)\,B_{42}\}^2}{(E_{30}-E_{20})}. \quad (A9)$$

By considering corrections up to the second-order, the approximation of the eigenvalues to the perturbed states becomes

$$E_i=E_{i0}+E_{i2}. \quad (A10)$$

Perturbation theory also gives the first correction eigenstates in C_{2v} symmetry [9].

$$\Phi_1=a_1|\pm 5/2\rangle+a_2|\mp 3/2\rangle+a_5|\pm 1/2\rangle,$$
$$\Phi_2=a_3|\pm 5/2\rangle+a_4|\mp 3/2\rangle+a_6|\pm 1/2\rangle, \quad (A11)$$
$$\Phi_3=a_7|\pm 5/2\rangle+a_8|\mp 3/2\rangle+a_9|\pm 1/2\rangle.$$

The perturbed eigenstates of (A 11) are normalised but not orthogonal, and the coefficients a_i are functions of the crystal field intensity parameters B_{kq}.

2. Zeeman Energy

The Zeeman energy in an applied magnetic field is described by the Hamiltonian

$$\hat{H}_M=-g\,\mu_B\,\hat{J}\cdot\hat{H}=-g\,\mu_B(J_x H_x+J_y H_y+J_z H_z), \quad (A12)$$

where g is the Landé factor (6/7 in this case), μ_B the Bohr magneton, $\hat{J}$ the operator of the total angular

Table A 3. Zeeman energies in an applied field ($G = g\,\mu_B\,H$).

1st order Zeeman effect		2nd order Zeeman effect	
E_z	Φ_1	$\pm\frac{1}{2}(5\,a_1^2-3\,a_2^2+a_5^2)\,G$	$E_z\,\Phi_1$	$-\frac{1}{4}\left\{\frac{(5\,a_1\,a_3-3\,a_2\,a_4+a_5\,a_6)^2}{E_2-E_1}+\frac{(5\,a_1\,a_7-3\,a_2\,a_8+a_9\,a_5)^2}{E_3-E_1}\right\}G^2$
	Φ_2	$\pm\frac{1}{2}(5\,a_3^2-3\,a_4^2+a_6^2)\,G$	Φ_2	$\frac{1}{4}\left\{\frac{(5\,a_1\,a_3-3\,a_2\,a_4+a_5\,a_6)^2}{E_2-E_1}-\frac{(5\,a_3\,a_7-3\,a_4\,a_8+a_6\,a_9)^2}{E_3-E_2}\right\}G^2$
	Φ_3	$\pm\frac{1}{2}(5\,a_7^2-3\,a_8^2+a_9^2)\,G$	Φ_3	$\frac{1}{4}\left\{\frac{(5\,a_1\,a_7-3\,a_2\,a_8+a_5\,a_9)^2}{E_3-E_1}+\frac{(5\,a_3\,a_7-3\,a_4\,a_8+a_6\,a_9)^2}{E_3-E_2}\right\}G^2$
E_x	Φ_1	$\pm(\sqrt{5}\,a_1\,a_2+2\sqrt{2}\,a_2\,a_5+3\,a_5^2/2)\,G$	$E_x\,\Phi_1$	$-\frac{1}{4}\left\{\frac{(\sqrt{5}\,(a_1\,a_4+a_2\,a_3)+2\sqrt{2}\,(a_2\,a_6+a_4\,a_5)+3\,a_5\,a_6)^2}{E_2-E_1}+\frac{(\sqrt{5}\,(a_1\,a_8+a_2\,a_7)+2\sqrt{2}\,(a_2\,a_6+a_4\,a_5)+3\,a_5\,a_6)^2}{E_3-E_1}\right\}G^2$
	Φ_2	$\pm(\sqrt{5}\,a_3\,a_4+2\sqrt{2}\,a_4\,a_6+3\,a_6^2/2)\,G$	Φ_2	$\frac{1}{4}\left\{\frac{(\sqrt{5}\,(a_1\,a_4+a_2\,a_3)+2\sqrt{2}\,(a_2\,a_6+a_4\,a_5)+3\,a_5\,a_6)^2}{E_2-E_1}-\frac{(\sqrt{5}\,(a_3\,a_8+a_4\,a_7)+2\sqrt{2}\,(a_4\,a_9+a_8\,a_6)+3\,a_6\,a_9)^2}{E_3-E_2}\right\}G^2$
	Φ_3	$\pm(\sqrt{5}\,a_7\,a_8+2\sqrt{2}\,a_8\,a_9+3\,a_9^2/2)\,G$	Φ_3	$\frac{1}{4}\left\{\frac{(\sqrt{5}\,(a_1\,a_8+a_2\,a_7)+2\sqrt{2}\,(a_2\,a_6+a_4\,a_5)+3\,a_5\,a_6)^2}{E_3-E_1}+\frac{(\sqrt{5}\,(a_3\,a_8+a_4\,a_7)+2\sqrt{2}\,(a_4\,a_9+a_8\,a_6)+3\,a_6\,a_9)^2}{E_3-E_2}\right\}G^2$
E_y	Φ_1	$\pm(\sqrt{5}\,a_1\,a_2-2\sqrt{2}\,a_2\,a_5+3\,a_5^2/2)\,G$	$E_y\,\Phi_1$	0
	Φ_2	$\pm(\sqrt{5}\,a_3\,a_4-2\sqrt{2}\,a_4\,a_6+3\,a_6^2/2)\,G$	Φ_2	0
	Φ_3	$\pm(\sqrt{5}\,a_7\,a_8-2\sqrt{2}\,a_8\,a_9+3\,a_9^2/2)\,G$	Φ_3	0

momentum with the components J_x, J_y, J_z, and $\hat{H}$ the applied magnetic field. Because of the anisotropy in C_{2v} point symmetry, the Zeeman energy along X, Y, and Z must be calculated separately. The Zeeman energies, up to second order and expressed in terms of the parameters a_i and G ($=g\,\mu_B H$), are given in Table A 3. Two points should be mentioned here. First, in calculating Zeeman energies using perturbation theory, the influence of all the other states should be considered because the perturbed eigenstates in (A 11) are not orthonormal. Second, for calculating the Zeeman energies of E_x and E_y, degenerate perturbation theory [9] was used because the matrix elements of $\langle|H_{Mx}|\rangle$ and $\langle|H_{My}|\rangle$ are nonzero between the degerate energy levels.

Acknowledgements

We thank Dr. K. Peters for the data collection, Mrs. E.-M. Peters for providing Fig. 1, Mr. M. Gehrke for the measurement of the magnetic susceptibility, and Mr. C.-S. Neumann for helpful discussion with the theoretical calculation.

[1] C.-S. Neumann and P. Fulde, Z. Phys. B-Condensed Matter **74,** 277 (1989).
[2] Mazhar-Ul-Haque, C. N. Caughlan, F. A. Hart, and R. Van Nice, Inorg. Chem. **10,** 115 (1971).
[3] D. R. Cousine and F. A. Hart, J. Inorg. Nucl. Chem. **29,** 1745 (1967).
[4] M. T. Hutchings, Point Charge Calculations of Energy Levels of Magnetic Ions in Crystalline Electric Field. In: Solid State Physics, Vol. 16, p. 254 (S. Frederick and T. David, eds.). Academic Press, New York 1964.
[5] A. J. Freeman and R. E. Watson, Phys. Rev. **127,** 2058 (1962).
[6] H. Lueken, W. Brüggemann, W. Bronger, and J. Fleischauer, J. Less-comm. Met. **65,** 79 (1979).
[7] M. T. Hutchings, Solid State Phys. **16,** 227 (1964).
[8] K. W. H. Stevens, Proc. Phys. Soc. London, Sect. A **65,** 209 (1952).
[9] I. N. Lavine, Quantum Chemistry, 2nd edition, p. 178, Allyn and Bocon, Inc., Boston 1975.
[10] H. Werner, Magnetochemie, p. 96, Akademie-Verlag, Berlin 1968.